

Description of the isotope chain $^{180-196}\text{Pt}$ within several solvable approaches

A. A. Raduta^{1,2} and P. Buganu¹¹*Department of Theoretical Physics, Institute of Physics and Nuclear Engineering, Post Office Box MG6, Bucharest 077125, Romania*²*Academy of Romanian Scientists, 54 Splaiul Independentei, Bucharest 050094, Romania*

(Received 15 October 2013; revised manuscript received 9 December 2013; published 30 December 2013)

Energies of the ground, β and γ bands as well as the associated $B(E2)$ values are determined for each even-even isotope of the $^{180-196}\text{Pt}$ chain by the exact solutions of some differential equations which approximate the generalized Bohr-Mottelson Hamiltonian. The emerging approaches are called the sextic and spheroidal approach (SSA), the sextic and Mathieu approach (SMA), the infinite square well and spheroidal approach (ISWSA), and the infinite square well and Mathieu approach (ISWMA). While the first three methods were formulated in some earlier papers, ISWMA is an unedited approach of this work. Numerical results are compared with those obtained with the so-called X(5) and Z(5) models. A contour plot for the probability density as function of the intrinsic dynamic deformations is given for a few states of the three considered bands with the aim of evidencing the shape evolution along the isotope chain and pointing out possible shape coexistence.

DOI: [10.1103/PhysRevC.88.064328](https://doi.org/10.1103/PhysRevC.88.064328)

PACS number(s): 21.10.Re, 21.60.Ev, 27.70.+q

I. INTRODUCTION

Since the critical point symmetries [1–5] of the nuclear shape phase transitions were proposed, many experimental and theoretical efforts were made to find the nuclei described by the new symmetries. While at the beginning the X(5) [3] candidates were found in the mass region of $A \approx 150$ [6–8], recently a new region has been suggested for Os and Pt isotopes with $A \approx 180$ [9,10]. In Refs. [11,12] data for the isotopes $^{176,178,180,188,190,192}\text{Os}$ were analyzed with the sextic and spheroidal approach (SSA) [11], the Davidson and spheroidal approach (DSA) [12], and the infinite square well and spheroidal approach (ISWSA) [13], and the results were compared with those of the coherent state model (CSM) [14] and X(5). According to our analysis these isotopes present features for the $U(5) \rightarrow SU(3)$ shape phase transition with the critical point reached for ^{176}Os and ^{188}Os . On the other hand, by applying the sextic and Mathieu approach (SMA) [15] to $^{188,190,192}\text{Os}$, we see that the isotope ^{192}Os is a good candidate for the critical point of the phase transition between the prolate and the oblate shapes through the triaxial shape corresponding to $\gamma_0 = 30^\circ$.

Encouraged by the results for the Os isotopes, we consider the above-mentioned models also for the even-even $^{180-196}\text{Pt}$ isotopes. We aim not only at determining the energy spectra and the electric transition probabilities but also at showing the static deformation of each isotope in both the ground and excited states. Features like shape coexistence or a transition from the prolate to oblate shapes through a triaxial deformation are expected to show up. Keeping in mind that the SMA, the ISWMA, and the Z(5) [5] are suitable for the description of the triaxial nuclei lying close to $\gamma_0 = 30^\circ$, a comparison of their predictions represents a challenging task. ISWMA is the unedited model proposed in this paper.

Recently, in Ref. [10] it was shown that the isotope ^{182}Pt has some of the X(5) features. According to the interacting boson model-1 (IBM-1) [16] and the general collective model [17], this isotope manifests shape coexistence and is close to the critical point of the $U(5) \rightarrow SU(3)$ shape phase transition.

Evidence for shape coexistence was also presented for $^{176,178}\text{Pt}$ [18,19], ^{184}Pt [20], ^{186}Pt [21], and ^{188}Pt [22], which suggests that this behavior is a specific feature for Pt isotopes. Some investigations where the ground-state shape evolution in Pt isotope chain from the prolate towards the oblate shapes were performed in Refs. [23,24].

The objectives formulated above are achieved according to the following plan. In Sec. II, a short presentation of the formalisms used for the description of the Pt even-even isotopes is given. Numerical results and their comparison with the corresponding experimental data are discussed in Sec. III. The final conclusions are drawn in Sec. IV.

II. SHORT PRESENTATION OF THE MODELS

The formalisms X(5), Z(5), ISWSA, ISWMA, SSA, and SMA are derived by a set of approximations applied to the Bohr-Mottelson Hamiltonian [1],

$$H = -\frac{\hbar^2}{2B} \left[\frac{1}{\beta^4} \frac{\partial}{\partial \beta} \beta^4 \frac{\partial}{\partial \beta} + \frac{1}{\beta^2 \sin 3\gamma} \frac{\partial}{\partial \gamma} \sin 3\gamma \frac{\partial}{\partial \gamma} - \frac{1}{4\beta^2} \sum_{k=1}^3 \frac{\hat{Q}_k^2}{\sin^2(\gamma - \frac{2\pi}{3}k)} \right] + C \frac{\beta^2}{2}, \quad (2.1)$$

amended with a potential [25,26]

$$V(\beta, \gamma) = V_1(\beta) + \frac{V_2(\gamma)}{\beta^2}. \quad (2.2)$$

The form of the β and γ potential allows us to separate the β variable from the γ and the three Euler angles θ_1 , θ_2 , and θ_3 . Here, \hat{Q}_k 's denote the angular momentum components in the intrinsic reference frame. A full separation, however, may be achieved by expanding the rotor term in power series of γ around either of $\gamma_0 = 0$ or of $\gamma_0 = \pi/6$ and, moreover, by replacing the factor β^2 multiplying the γ -dependent term with

its average value, denoted hereafter by $\langle \beta^2 \rangle$. The resulting equations are

$$\left[-\frac{1}{\beta^4} \frac{d}{d\beta} \beta^4 \frac{d}{d\beta} + \frac{\Lambda}{\beta^2} + v_1(\beta) \right] f(\beta) = \varepsilon_\beta f(\beta), \quad (2.3)$$

$$\left[-\frac{1}{\sin 3\gamma} \frac{d}{d\gamma} \sin 3\gamma \frac{d}{d\gamma} - W + v_2(\gamma) \right] \phi(\gamma) = \tilde{\varepsilon}_\gamma \phi(\gamma), \quad (2.4)$$

where the following notations are used:

$$v_1(\beta) = \frac{2B}{\hbar^2} V_1(\beta), \quad v_2(\gamma) = \frac{2B}{\hbar^2} V_2(\gamma),$$

$$\varepsilon_\beta = \frac{2B}{\hbar^2} E_\beta, \quad \tilde{\varepsilon}_\gamma = \langle \beta^2 \rangle \frac{2B}{\hbar^2} E_\gamma. \quad (2.5)$$

Λ and W are the contributions coming from the rotor term and their expressions depend on the order of the γ series truncation.

For the sake of fixing the notations and defining the main ingredients, in what follows the above-mentioned approaches will be briefly described. For details we advise the reader to consult Refs. [3,5,11–13,15,25,26]. In Eq. (2.3), the X(5), Z(5), ISWSA, and ISWMA models use a common potential in β , namely an infinite square well:

$$v_1(\beta) = \begin{cases} 0, & \beta \leq \beta_\omega \\ \infty, & \beta > \beta_\omega. \end{cases} \quad (2.6)$$

With such a choice Eq. (2.3) admits the Bessel functions of irrational order ν , as solutions:

$$f_{s,L}(\beta) = C_{s,L} \beta^{-\frac{3}{2}} J_\nu \left(\frac{x_{s,L}}{\beta_\omega} \beta \right), \quad s = 1, 2, 3, \dots \quad (2.7)$$

$C_{s,L}$ denotes the normalization factor, $x_{s,L}$ are the Bessel function zeros, while L is the total intrinsic angular momentum.

By contrast the SSA and SMA use in Eq. (2.3) a sextic oscillator plus a centrifugal barrier potential [27],

$$v_1^\pm(\beta) = (b^2 - 4ac^\pm)\beta^2 + 2ab\beta^4 + a^2\beta^6 + u_0^\pm,$$

$$c^\pm = \frac{L}{2} + \frac{5}{4} + M, \quad M = 0, 1, 2, \dots \quad (2.8)$$

Here, c^\pm has two different values, one for L even and other for L odd, while u_0^\pm are constants which are fixed such that the two potentials v_1^+ and v_1^- have the same minimum energy. Equation (2.3), with $\Lambda = L(L+1) - 2$ and the potential given by Eq. (2.8), is quasixactly solved, the solutions being of the form

$$\varphi_{n_\beta,L}^{(M)}(\beta) = N_{n_\beta,L} P_{n_\beta,L}^{(M)}(\beta^2) \beta^{L+1} e^{-\frac{a}{4}\beta^4 - \frac{b}{2}\beta^2},$$

$$n_\beta = 0, 1, 2, \dots, M, \quad (2.9)$$

where $N_{n_\beta,L}$ is the normalization factor, while $P_{n_\beta,L}^{(M)}(\beta^2)$ are polynomials of order n_β in β^2 .

Concerning Eq. (2.4), X(5) and Z(5) chose an oscillator and a shifted oscillator potential, respectively:

$$v_2(\gamma) = c \frac{1}{2} (\gamma - \gamma_0)^2. \quad (2.10)$$

Indeed, for X(5) $\gamma_0 = 0$ and the solutions of Eq. (2.4) are the generalized Laguerre polynomials, L_n^m :

$$\eta_{n_\gamma,K}(\gamma) = C_{n,K} \gamma^{|K|/2} e^{-(3a)\gamma^2/2} L_n^{|K|}(3a\gamma^2),$$

$$n = \left(\frac{n_\gamma - |K|}{2} \right), \quad a = \frac{\sqrt{c}}{3}, \quad n_\gamma = 0, 1, 2, \dots \quad (2.11)$$

The quantum number K corresponds to the angular momentum projection on the intrinsic z axis. As for Z(5), $\gamma_0 = \pi/6$ and the corresponding equation (2.4) is obeyed by the Hermite polynomials H_n :

$$\eta_{\bar{n}_\gamma} = N_{\bar{n}_\gamma} H_{\bar{n}_\gamma} [b(\gamma - \pi/6)] e^{-b^2(\gamma - \pi/6)^2/2},$$

$$b = \left(\frac{c\langle \beta^2 \rangle}{2} \right)^{1/4}, \quad \bar{n}_\gamma = 0, 1, 2, \dots \quad (2.12)$$

Both models, the X(5) and the Z(5), consider in Eq. (2.4) a zeroth order of approximation for the rotor term.

This is not the case for the ISWSA, ISWMA, SSA, and SMA models, where a second-order power expansion of both the rotor term and the periodic potential

$$v_2(\gamma) = u_1 \cos 3\gamma + u_2 \cos^2 3\gamma \quad (2.13)$$

is used, which results in having the spheroidal ($S_{m,n}$) and Mathieu (\mathcal{M}_n) functions as solutions of the resulting differential equations, respectively:

$$\eta(\gamma) = S_{m,n}(\cos 3\gamma; c), \quad \eta(\gamma) = \frac{\mathcal{M}_n(3\gamma; q)}{\sqrt{|\sin 3\gamma|}}. \quad (2.14)$$

The expressions of c and q are specified below.

The advantages of the Mathieu and spheroidal functions are that they are periodic, defined on a bound interval, and normalized to unity with the integration measure of $|\sin 3\gamma| d\gamma$, preserving in this way the hermiticity of the initial Hamiltonian. Note that the other approaches do not satisfy these conditions.

The total energy of the system is obtained by summing the eigenvalues of the β and γ equations:

$$\varepsilon = \varepsilon_\beta + \tilde{\varepsilon}_\gamma. \quad (2.15)$$

The excitation energies yielded by the formalisms used in the present paper are as follows:

$$\mathbf{X}(5): E(s, L, n_\gamma, K) - E(1, 0, 0, 0) = B_1(x_{s,L}^2 - x_{1,0}^2) + \delta_{K,2} X,$$

$$X = A_1 + 4C_1, \quad (2.16)$$

with A_1 , B_1 , and C_1 arbitrary parameters. In our calculations the parameter X is fitted.

$$\mathbf{Z(5):} \quad E(s, L, n_\gamma = 0, R) - E(1, 0, 0, 0) = B_1(x_{s,L,R}^2 - x_{1,0,0}^2), \quad B_1 = \frac{1}{\beta_\omega^2} \frac{\hbar^2}{2B}, \quad (2.17)$$

$$\begin{aligned} \mathbf{ISWSA:} \quad E(s, n_\gamma, m_\gamma, L, K) &= B_1 x_{s,L}^2 + F \left[9\lambda_{m_\gamma, n_\gamma}(c) + \frac{u_1}{2} + \frac{11}{27}D - \frac{L(L+1)}{3} \right], \\ \lambda_{m_\gamma, n_\gamma} &= \frac{1}{9} \left[\tilde{\varepsilon}_\gamma - \frac{u_1}{2} - \frac{11}{27}D + \frac{1}{3}L(L+1) \right], \quad c^2 = \frac{1}{9} \left(\frac{u_1}{2} + u_2 - \frac{2}{27}D \right), \\ m_\gamma &= \frac{K}{2}, \quad D = L(L+1) - K^2 - 2, \quad F = \frac{1}{\langle \beta^2 \rangle} \frac{\hbar^2}{2B}, \end{aligned} \quad (2.18)$$

$$\begin{aligned} \mathbf{ISWMA:} \quad E(s, n_\gamma, L, R) &= B_1 x_{s,L}^2 + F \left[9a_{n_\gamma}(L, R) + 18q(L, R) - \frac{3}{4}R^2 - \frac{5}{2} \right], \\ q &= \frac{1}{36} \left(\frac{10}{9}L(L+1) - \frac{13}{12}R^2 + u_1 - \frac{9}{4} \right), \quad a_{n_\gamma} = \frac{1}{9} \left(\tilde{\varepsilon}_\gamma + \frac{3}{4}R^2 + \frac{5}{2} \right) - 2q, \end{aligned} \quad (2.19)$$

$$\begin{aligned} \mathbf{SSA:} \quad E(n_\beta, n_\gamma, m_\gamma, L, K) &= G \left[b(2L+3) + \lambda_{n_\beta}^{(M)} + u_0^\pm \right] + F \left[9\lambda_{m_\gamma, n_\gamma}(c) + \frac{u_1}{2} + \frac{11}{27}D - L(L+1) \right], \\ \lambda_{m_\gamma, n_\gamma} &= \frac{1}{9} \left[\tilde{\varepsilon}_\gamma - \frac{u_1}{2} - \frac{11}{27}D + \frac{1}{3}L(L+1) \right] + \frac{2L(L+1)}{27}, \quad G = \frac{\hbar^2}{2B}, \end{aligned} \quad (2.20)$$

$$\mathbf{SMA:} \quad E(n_\beta, n_\gamma, L, R) = G \left[4bs(L) + \lambda_{n_\beta}^{(M)}(L) + u_0^\pi \right] + F \left[9a_{n_\gamma}(L, R) + 18q(L, R) - \frac{3}{4}R^2 - \frac{5}{2} \right], \quad (2.21)$$

where $\lambda_{n_\beta}^{(M)}(L)$ satisfy the equation

$$\left[- \left(\frac{d^2}{d\beta^2} + \frac{4s-1}{\beta} \frac{d}{d\beta} \right) + 2b\beta \frac{d}{d\beta} + 2a\beta^2 \left(\beta \frac{d}{d\beta} - 2M \right) \right] P_{n_\beta, L}^{(M)}(\beta^2) = \lambda_{n_\beta}^{(M)} P_{n_\beta, L}^{(M)}(\beta^2). \quad (2.22)$$

The specific β and γ potentials of the six approaches used in the present paper are collected, for comparison, in Table I. The potentials in the β variable are to be amended by a centrifugal term due to the rotor component of the starting Hamiltonian.

The reduced $E2$ transition probabilities for ISWSA and SSA are determined with the reduced matrix element of the transition operator,

$$T_{2\mu}^{(E2)} = t_1 \beta \left[\cos \gamma D_{\mu 0}^2 + \frac{\sin \gamma}{\sqrt{2}} (D_{\mu 2}^2 + D_{\mu, -2}^2) \right] + t_2 \sqrt{\frac{2}{7}} \beta^2 \left[-\cos 2\gamma D_{\mu 0}^2 + \frac{\sin 2\gamma}{\sqrt{2}} (D_{\mu 2}^2 + D_{\mu, -2}^2) \right], \quad (2.23)$$

TABLE I. Here we list the β and γ potentials used by the approaches ISWSA, SSA, ISWMA, and SMA. For comparison the potentials characterizing X(5) and Z(5) are also given.

Approach	β potential	γ potential
X(5)	0, for $\beta \leq \beta_\omega$; ∞ , for $\beta > \beta_\omega$.	$\frac{\varepsilon}{2} \gamma^2$.
Z(5)	0, for $\beta \leq \beta_\omega$; ∞ , for $\beta > \beta_\omega$.	$\frac{\varepsilon}{2} (\gamma - \frac{\pi}{6})^2$.
ISWSA	0, for $\beta \leq \beta_\omega$; ∞ , for $\beta > \beta_\omega$.	$u_1 \cos 3\gamma + u_2 \cos^2 3\gamma + \frac{9}{4 \sin^2 3\gamma}$.
SSA	$(b^2 - 4ac^\pm)\beta^2 + 2ab\beta^4 + a^2\beta^6 + u_0^\pm$, $c^\pm = \frac{L}{2} + \frac{5}{4} + m$; $m = 0, 1, 2, \dots$	$u_1 \cos 3\gamma + u_2 \cos^2 3\gamma + \frac{9}{4 \sin^2 3\gamma}$.
ISWMA	0 for $\beta \leq \beta_\omega$; ∞ , for $\beta > \beta_\omega$.	$-2q \cos 6\gamma$; $q = \frac{1}{36} \left(\frac{10}{9}L(L+1) - \frac{13}{12}R^2 + \mu - \frac{9}{4} \right)$.
SMA	$(b^2 - 4ac^\pm)\beta^2 + 2ab\beta^4 + a^2\beta^6 + u_0^\pm$, $c^\pm = \frac{L}{2} + \frac{5}{4} + m$; $m = 0, 1, 2, \dots$	$-2q \cos 6\gamma$; $q = \frac{1}{36} \left(\frac{10}{9}L(L+1) - \frac{13}{12}R^2 + \mu - \frac{9}{4} \right)$.

between the corresponding initial $|L_i M_i\rangle$ and final $|L_f M_f\rangle$ states, as described above:

$$B(E2; L_i \rightarrow L_f) = |\langle L_i || T_2^{(E2)} || L_f \rangle|^2. \quad (2.24)$$

Here Rose's convention [28] was used for the reduced matrix elements. For SMA, ISWMA, and Z(5), in the expression of the transition operator (2.23) γ is substituted with $\gamma - 2\pi/3$. The argument is justified by the fact that $\gamma - 2\pi/3$ defines the axis 1 of the principal inertial ellipsoid. Indeed, the transformation from the laboratory to the intrinsic frame is a rotation defined by the matrix D_{MR}^L , where M and R are eigenvalues of the operator \hat{Q}_1 . The X(5) and Z(5) models keep only the zeroth-order approximation of the first γ term in the transition operator (2.23).

III. NUMERICAL RESULTS

The formalisms presented in Sec. II were applied to some even-even isotopes of Pt: $^{180-196}\text{Pt}$. It is commonly accepted that nuclear spectra can be classified by the values of the energy ratios:

$$R_{4_g^+/2_g^+} = \frac{E_{4_g^+} - E_{0_g^+}}{E_{2_g^+} - E_{0_g^+}}, \quad R_{0_\beta^+/2_g^+} = \frac{E_{0_\beta^+} - E_{0_g^+}}{E_{2_g^+} - E_{0_g^+}}. \quad (3.1)$$

Moreover, it seems that nuclei satisfying a certain symmetry are characterized by almost constant ratios. The values of these ratios associated to the isotopes considered here are collected in Table II. As seen from there, the ratios $R_{4_g^+/2_g^+}$ for $^{180,182,184}\text{Pt}$ are close to that predicted by the X(5) approach. By contrast the other ratio $R_{0_\beta^+/2_g^+}$ indicates that these isotopes are far from the ideal picture of X(5). As a matter of fact this feature is consistent with the results of Ref. [29] that not all nuclear properties reach the critical point in a phase transition in the same isotope. We apply the approaches ISWSA and SSA to the mentioned isotopes in order to test their ability to account for these complementary features.

Concerning the description called Z(5) this is appropriate for $^{190,192,194,196}\text{Pt}$, the statement being supported by the values of both ratios. Indeed, the detailed numerical analysis of Ref. [5] shows a good agreement between calculations and experimental data. In this context the application of the ISWMA and SMA to these isotopes will provide a sensible comparison of the formalisms on one hand and Z(5) on the other hand.

It is well known that the triaxial rigid rotor (TRR) predicts [30] a relation between the first three excited state energies:

$$\Delta E \equiv E_{3_\gamma^+} - E_{2_\gamma^+} - E_{2_g^+} = 0. \quad (3.2)$$

Due to this fact, the above equation is considered to be a signature for a triaxial deformation of $\gamma_0 = 30^\circ$. For the

isotope ^{192}Pt the above equation reads $|\Delta E| = 8$ keV, which means that the mentioned isotope is close to the ideal triaxial rigid rotor. Considering this isotope among the treated isotopes allows us to answer the question of whether these approaches are suitable for the description of the triaxial nuclei. The isotopes $^{186,188,190,192,194,196}\text{Pt}$ may be considered to be γ -unstable nuclei, having the ratio $R_{4_g^+/2_g^+}$ close to 2.5. A special case is that of ^{186}Pt , which has the head state of γ band higher in energy than the first β state, which results in claiming a γ stable picture. Most likely this nucleus exhibits the main features for the critical point of the phase transition from prolate to oblate shapes. Due to the specific structure of their potentials in the γ variable, ISWSA and SSA seem to be suitable to describe both the γ -unstable and γ -stable deformed nuclei. Actually this argument justifies including ^{186}Pt and ^{188}Pt on the list of considered isotopes. In addition to the prolate-oblate transition along the Pt isotopic chain an alternative prolate-oblate transition has been considered in Ref. [31], with both transitions studied in Ref. [32].

Each approach involves a number of free parameters for energies as well as for $B(E2)$ values. These are fixed by fitting some particular experimental data concerning either the excitation energies or the reduced transition probabilities. The results of the fitting procedure adopted are listed in Tables III and IV. As seen from these tables, the number of parameters used for fitting the spectra in X(5), ISWSA, and SSA are 2, 4, and 6, respectively, while in the fitting of $B(E2)$ values 1, 2, and 2 parameters are used, respectively. Also, from Table III we notice that the number of parameters used for fitting the spectra in Z(5), ISWMA, and SMA are 1, 3, and 5, respectively, while in fitting the $B(E2)$ s 1, 2, and 2 parameters are used, respectively.

Numerical results for the excitation energies of the ground, β , and γ bands, as well as for the quadrupole electric transitions between states of these bands, are compared with the corresponding experimental data in Tables V and VI, respectively. For each formalism the agreement between the calculation results and the corresponding experimental data is quantitatively appraised by the rms values of the deviations.

From Table V, one can see that spectra of the isotopes ^{180}Pt , ^{182}Pt , and ^{184}Pt are better described by SSA and ISWSA than by X(5). The best approach seems to be SSA. Moreover, the X(5) failure in explaining the data from the β band is removed by SSA, and that happens especially for ^{182}Pt . Concerning the γ band, all three formalisms, SSA, ISWSA, and X(5), encounter difficulties in explaining the bandhead energy. A possible explanation would be that the state 2_γ^+ does not actually belong to the γ band. In this context we mention the fact that two alternative interpretations have been

TABLE II. Signatures of X(5), Z(5), and O(6) symmetries identified in the even-even isotopes $^{180-196}\text{Pt}$. The two ratios are defined by Eq. (3.1).

	^{180}Pt	^{182}Pt	^{184}Pt	^{186}Pt	^{188}Pt	^{190}Pt	^{192}Pt	^{194}Pt	^{196}Pt	X(5)	Z(5)	O(6)
$R_{4_g^+/2_g^+}$	2.69	2.71	2.67	2.55	2.52	2.49	2.48	2.47	2.46	2.90	2.35	2.50
$R_{0_\beta^+/2_g^+}$	3.12	3.23	3.02	2.46	3.00	3.11	3.78	3.86	3.19	5.65	3.91	

TABLE III. The parameters characterizing the X(5), ISWSA, and SSA approaches, determined by a fitting procedure, are listed for $^{180-188}\text{Pt}$ isotopes.

Nucl	B_1 (keV)		X (keV)			F (keV)		u_1		u_2		G (keV)	a			b			t_1 (W.u.) $^{1/2}$			t_2 (W.u.) $^{1/2}$		
	X(5)	ISWSA	X(5)	ISWSA	SSA	ISWSA	SSA	ISWSA	SSA	SSA	SSA		SSA	SSA	X(5)	ISWSA	SSA	ISWSA	SSA	X(5)	ISWSA	SSA	ISWSA	SSA
^{180}Pt	19.08	16.38	722.5	17.32	3.34	-0.15	-821.2	-104.6	-1000	1.04	1059	135	500.2	614.4	1750	0.0	0.0							
^{182}Pt	18.02	16.39	720.7	11.33	5.33	-31.56	-1042	-163	-0.0007	0.81	1687	186	451.2	2200	6561	9062	89567							
^{184}Pt	17.28	16.83	739.7	3.35	6.25	-1000	-302.6	-1000	-262	0.62	3030	256	419.6	2422	7821	11331	122065							
^{186}Pt		16.25		16.82	3.08	-253.87	1471	6.75	-2326	0.85	1296	170		1728	5061	5978	58515							
^{188}Pt		21.5		41.99	14.55	-97.45	-466.2	81.07	165.8	1.45	1449	95		517.4	1717	0.0	0.0							

studied in Ref. [42] with a related description appearing in Ref. [43]. A similar situation is met in ^{186}Pt . In ^{188}Pt , however, all three bands considered here are realistically described by SSA.

The comparison of the numerical results yielded by SMA, ISWMA, and Z(5) with experimental data for the even-even isotopes $^{190-196}\text{Pt}$, is made also in Table V, with the result in favor of SMA and ISWMA.

The electromagnetic transition probabilities, calculated with Eq. (2.24), are included in Table VI. By analyzing the rms values for each model, one may conclude that SSA and ISWSA describe the experimental data better than X(5), while SMA and ISWMA describe the data better than Z(5). An explanation for this could be that X(5) and Z(5) use only the zeroth-order approximation of the harmonic part of the transition operator (2.23). Indeed, as shown in Table VI, for ^{180}Pt the results obtained by SSA and ISWSA using only the harmonic transition operator are almost identical with those of X(5). By contrast for $^{182,184}\text{Pt}$, where the anharmonic contributions were included, the results of SSA and ISWSA are better than those of X(5). It is worth noticing that the rms associated to Z(5) for ^{192}Pt and ^{196}Pt are smaller than those provided by ISWMA. This situation might be caused by the fact the two approaches considered for the γ band have different descriptions. Indeed, in the framework of Z(5) the states of γ band are characterized by $n_\gamma = 0$, while the ISWMA γ states have $n_\gamma = 1$.

In Table VII we list the results for branching ratios of few states from the γ and β bands obtained by SSA, ISWSA, SMA, and ISWMA approaches, respectively. They are compared with the experimental data of Ref. [40]. For $^{190,192,194}\text{Pt}$ we list also the results yielded by the Z(5) formalism. The parameters determining the transition operator were fixed as follows: For

^{188}Pt and ^{190}Pt we kept t_1 as given in Tables III and IV, respectively, while t_2 was fixed by a least square procedure. The results for t_2 are also listed in Table VII. As for the rest of isotopes from the table, the parameters t_1, t_2 are as listed in Tables III and IV.

Another objective of the present work is to determine the isotope shape in ground and excited states, within both the SSA and the SMA. Indeed, it is interesting to see how the shape changes when one passes from one isotope to another and moreover whether this picture is state dependent. We expect to visualize the shape phase transition and also possible shape coexistence. The static shape is defined by the values of the intrinsic variables β and γ for which the probability density (the probability in the volume unit of $d\beta d\gamma$),

$$P(\beta, \gamma) = |f(\beta)\phi(\gamma)|^2 \beta^4 |\sin 3\gamma|, \quad (3.3)$$

reaches a maximum value. In Fig. 1, the contour plots are represented in the coordinates $(\beta \cos \gamma, \beta \sin \gamma)$. In order to save the space we chose two representatives for SSA, ^{180}Pt and ^{188}Pt , and one for SMA, ^{190}Pt . Indeed, the graphs corresponding to $^{182-186}\text{Pt}$ are similar to that of ^{180}Pt and those of $^{192-196}\text{Pt}$ resemble that of ^{190}Pt . We may ask ourselves why we make such plots once we know that the power expansion in γ was performed around $\gamma = 0^\circ$ and $\gamma = 30^\circ$. We notice that the density maxima are met not in the same point where the potential is minimum. The reason is that the density accounts also for the kinetic energy and moreover includes a factor defining the measure of the integration in the β and γ coordinates. These figures reflect the structure of the wave functions. Indeed, since the γ -dependent function depends on $\cos 3\gamma$ and the spheroidal functions are symmetric with respect to the space reflection transformation, the graphs exhibit the symmetry $\gamma \rightarrow \pi/3 - \gamma$. Concerning SMA, the

TABLE IV. The parameters characterizing the Z(5), ISWMA, and SMA approaches, determined by a fitting procedure, are listed for $^{190-196}\text{Pt}$ isotopes.

Nucl	B_1 (keV)		F (keV)		u_1		G (keV)	a	b	t_1 (W.u.) $^{1/2}$			t_2 (W.u.) $^{1/2}$		
	Z(5)	ISWMA	ISWMA	SMA	ISWMA	SMA				Z(5)	ISWMA	SMA	ISWMA	SMA	
^{190}Pt	28.12	16.73	12.82	8.14	26.67	104.6	1.11	3014.12	84.00	27.49	28.14	96.38	0.00	0.0	
^{192}Pt	29.45	17.84	13.98	7.87	9.49	121.8	2.95	616.5	22.98	23.94	24.51	55.10	102.4	1048	
^{194}Pt	32.65	19.87	18.43	14.68	5.00	32.74	2.96	733.0	33.05	18.76	16.94	43.42	137.6	968.6	
^{196}Pt	31.49	18.27	9.98	6.48	56.53	177.1	0.41	28322	250	20.77	19.79	130.2	172.9	7708	

TABLE VI. The reduced $E2$ transition probabilities determined with the SSA, ISWSA, and X(5) models for $^{180-188}\text{Pt}$ and SMA, ISWMA, and Z(5) for $^{190-196}\text{Pt}$, are compared with the corresponding experimental data taken from Refs. [21,33,35,37-41].

B(E2) [W.u.]	^{180}Pt		^{182}Pt		^{184}Pt		^{186}Pt		^{188}Pt		^{190}Pt		^{192}Pt		^{194}Pt		^{196}Pt																				
	Exp	SSA ISWSA X(5)	Exp	SSA ISWSA X(5)	Exp	SSA ISWSA X(5)	Exp	SSA ISWSA X(5)	Exp	SSA ISWSA X(5)	Exp	SMA ISWMA Z(5)	Exp	SSA ISWSA Z(5)	Exp	SSA ISWSA Z(5)	Exp	SMA ISWMA Z(5)																			
$2_g^+ \rightarrow 0_g^+$	110	106	106	108 $^{+7}_{-7}$	167	166	86	127 $^{+5}_{-5}$	176	179	75	113 $^{+8}_{-8}$	162	162	82	82	56 $^{+3}_{-3}$	56	56	57.2 $^{+1.2}_{-1.2}$	49	41	42	49.2 $^{+0.8}_{-0.8}$	25	20	26	26	40.6 $^{+0.2}_{-0.2}$	34	28	32					
$4_g^+ \rightarrow 2_g^+$	168	169	169	188 $^{+11}_{-11}$	226	222	138	210 $^{+8}_{-8}$	238	236	119	188 $^{+13}_{-13}$	232	228	136	131	86	95	89	89 $^{+5}_{-5}$	73	71	68	85 $^{+5}_{-5}$	37	34	41	41	60 $^{+0.9}_{-0.9}$	52	48	51					
$6_g^+ \rightarrow 4_g^+$	≥ 50	202	210	284 $^{+18}_{-18}$	232	224	171	226 $^{+12}_{-12}$	243	235	148	289 $^{+23}_{-23}$	254	248	171	162	119	138	123	70 $^{+30}_{-30}$	98	103	94	67 $^{+21}_{-21}$	51	49	57	57	73 $^{+4}_{-4}$	72	70	70					
$8_g^+ \rightarrow 6_g^+$		230	241	241	253 $^{+30}_{-30}$	221	196	271 $^{+18}_{-18}$	232	222	170	294 $^{+29}_{-29}$	260	253	200	186	144	169	148					50 $^{+14}_{-14}$	61	60	69	69	78 $^{+78}_{-78}$	87	85	84					
$10_g^+ \rightarrow 8_g^+$		255	265	266	266 $^{+21}_{-21}$	204	202	216	310 $^{+10}_{-10}$	214	205	187	304 $^{+26}_{-26}$	259	254	226	205	166	166					34 $^{+9}_{-9}$	70	68	77	77									
$12_g^+ \rightarrow 10_g^+$		278	285	286	158 $^{+18}_{-18}$	185	189	232	183 $^{+17}_{-17}$	193	188	201	255 $^{+26}_{-26}$	252	249	220	249	220																			
$14_g^+ \rightarrow 12_g^+$		300	301	302	113 $^{+11}_{-11}$	164	178	246	165 $^{+17}_{-17}$	171	173	213	225 $^{+21}_{-21}$	243	249																						
$16_g^+ \rightarrow 14_g^+$								143 $^{+17}_{-17}$	150	159	223	201 $^{+36}_{-36}$	232	246																							
$18_g^+ \rightarrow 16_g^+$								80 $^{+5}_{-5}$	129	147	231																										
$2_g^+ \rightarrow 0_g^+$																																					
$3_g^+ \rightarrow 2_g^+$																																					
$4_g^+ \rightarrow 2_g^+$																																					
$6_g^+ \rightarrow 2_g^+$																																					
$0_g^+ \rightarrow 0_g^+$																																					
$2_g^+ \rightarrow 0_g^+$																																					
$2_g^+ \rightarrow 4_g^+$																																					
$0_g^+ \rightarrow 2_g^+$																																					
$2_g^+ \rightarrow 2_g^+$																																					
$3_g^+ \rightarrow 2_g^+$																																					
$3_g^+ \rightarrow 4_g^+$																																					
$4_g^+ \rightarrow 2_g^+$																																					
$4_g^+ \rightarrow 4_g^+$																																					
$6_g^+ \rightarrow 4_g^+$																																					
$6_g^+ \rightarrow 6_g^+$																																					
rms (W.u.)			36	39	39	47	52	80	43	49	86	36	40																								

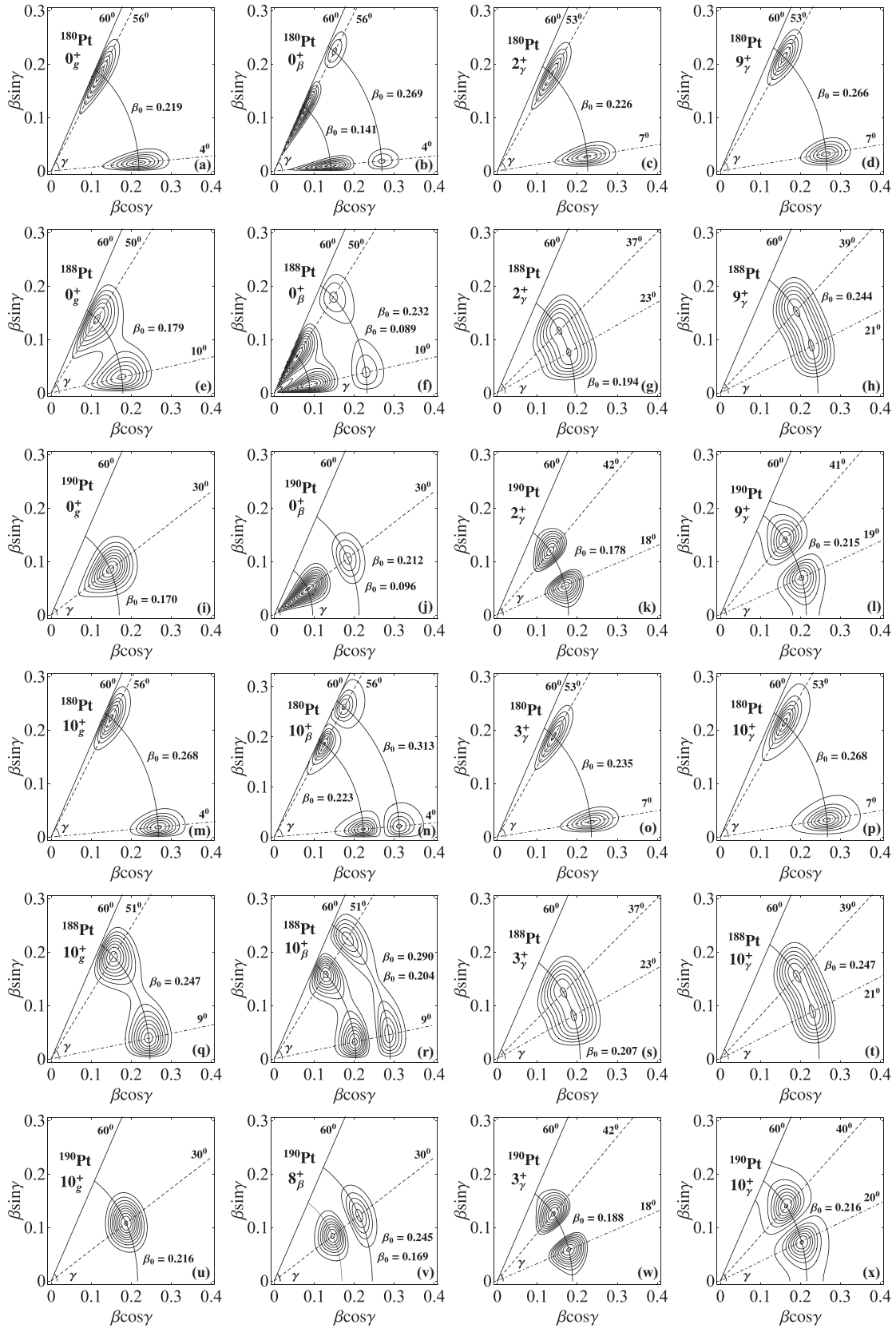


FIG. 1. Probability densities for the states 0_g^+ , 10_g^+ , 0_β , 10_β , 2_γ^+ , 3_γ^+ , 9_γ^+ , and 10_γ^+ of $^{180,188}\text{Pt}$ and ^{190}Pt , calculated with SSA and SMA, respectively. The steps used in the contour plots are 30, 10, and 20 for ^{180}Pt , ^{188}Pt , and ^{190}Pt , respectively. Exceptions are 0_β^+ for ^{188}Pt and 8_β^+ for ^{190}Pt , where the steps are 12 and 25, respectively.

TABLE VII. The branching ratios for some states of the ^{188}Pt and $^{190,192,194}\text{Pt}$ isotopes determined with SSA and ISWSA and SMA, ISWMA, and Z(5), respectively, are compared with the corresponding experimental data taken from Ref. [44].

$\frac{B(E2;J^+\rightarrow J'^+)}{B(E2;J^+\rightarrow J'^+)}$ $\times 10^2$	^{188}Pt			^{190}Pt				^{192}Pt				^{194}Pt			
	Exp.	SMA	ISWSA	Exp.	SMA	ISWMA	Z(5)	Exp.	SMA	ISWMA	Z(5)	Exp.	SMA	ISWMA	Z(5)
$2^+_{\gamma} \rightarrow 0^+_{\beta}$	3.44	63	66	1.24	1.95	4.90	0	0.51	1.96	7.55	0	0.38	1.81	2.01	0
$2^+_{\gamma} \rightarrow 2^+_{\beta}$															
$3^+_{\gamma} \rightarrow 2^+_{\beta}$	4.5	23	17	1.8	2.2	6.0	0	0.76	1.95	8.42	0	0.5	5.37	9.04	0
$3^+_{\gamma} \rightarrow 2^+_{\gamma}$															
$3^+_{\gamma} \rightarrow 4^+_{\beta}$		9.9	7.3	49	49	49	57	26	43	45	57		128	182	57
$3^+_{\gamma} \rightarrow 2^+_{\beta}$															
$0^+_{\beta} \rightarrow 2^+_{\beta}$	≥ 11	23.2	17	11	14	31	19	3.8	8.1	31	19	7.9	10.5	31	19
$0^+_{\beta} \rightarrow 0^+_{\beta}$															
$2^+_{\beta} \rightarrow 0^+_{\beta}$	0.83	0.37	3.17	0.02	0.82	0.02	1.39	0.022	1.16	0.017	1.39		1.04	0.02	1.39
$2^+_{\beta} \rightarrow 0^+_{\beta}$															
$2^+_{\beta} \rightarrow 4^+_{\beta}$	19	66	49	4.2	44	68	42	≤ 2.8	28	68	42		35	68	42
$2^+_{\beta} \rightarrow 0^+_{\beta}$															
r.m.s.		35	32		16	27	16		13	30	22		3	14	7
t_2 (W.u.) $^{\frac{1}{2}}$		-316.8	-184.9		2931	145.2									

mentioned symmetry is caused by the fact the potential in γ is function of $\cos^2 3\gamma$. Also, the node of the β function causes a doublet maxima with the same γ . For ^{188}Pt we notice equal density curves which surround two maxima of identical β . This situation is specific to the shape coexistence. It is worth mentioning that such transition is showing up despite the fact that for all isotopes $^{180-188}\text{Pt}$ we used a power expansion in γ around 0° . That means that the transition is caused not only by the potential shape but also by the structure coefficients involved in the associated differential equations. Actually, we calculated the spectroscopic properties of Pt isotopes with $A \geq 190$ also with a power expansion in γ around $\gamma = 0$. However, the results of SMA are characterized by smaller rms values for the deviations of the predictions from the experimental data. It is interesting to note that although we changed the description when we passed from ^{188}Pt to ^{190}Pt the probability density undergoes a smooth transition. The maxima surrounded by equidensity curves merge in one maximum at $\gamma = 30^\circ$ for ground and β band states, while for γ band states the doublets are well separated. How this picture is modified when additional degrees of freedom like octupole [45,46] or single particle [47,48] will be analyzed elsewhere.

Note that for ^{190}Pt the considered excited state in the β band is 8^+ and not 10^+ as happens for other isotopes. The reason is that, as seen from Table V, the highest spin state for which energies in nuclei with $A \geq 190$, calculated with SMA, is 8^+ .

IV. CONCLUSIONS

In the previous section we described some even-even isotopes of Pt by four solvable models emerging from the generalized Bohr Mottelson Hamiltonian. Indeed, for the isotopes with $180 \leq A \leq 188$ the approaches are those abbreviated by SSA and ISWSA, respectively, while for the rest of nuclei, $190 \leq A \leq 196$, the SMA and ISWMA are alternatively used. It is worth mentioning that the approach called ISWMA was used for the first time in the present paper. Since the first set exhibits some features of the X(5) ‘‘symmetry’’ we compared the results of our calculations with those obtained with the X(5) formalism, if they are available. As for the other isotopes the results were compared with the Z(5) results. One concludes that our results are slightly better than those obtained with X(5) and Z(5) methods regarding both the excitation energies and reduced $E2$ transition probabilities.

The wave function structure is nicely reflected in the contour plots for the probability density. It is suggested that due to the Hamiltonian symmetries the wave functions might be suitable for accounting for shape evolution as well as for possible shape coexistence.

ACKNOWLEDGMENT

This work was supported by the Romanian Ministry for Education Research Youth and Sport through the CNCSIS Project ID-2/5.10.2011.

- [1] A. Bohr, *Mat. Fys. Medd. Dan. Vid. Selsk.* **26**, 14 (1952); A. Bohr and B. Mottelson, *Mat. Fys. Medd. K. Dan. Vidensk. Selsk.* **27**, 15 (1953).
[2] F. Iachello, *Phys. Rev. Lett.* **85**, 3580 (2000).
[3] F. Iachello, *Phys. Rev. Lett.* **87**, 052502 (2001).
[4] F. Iachello, *Phys. Rev. Lett.* **91**, 132502 (2003).
[5] D. Bonatsos, D. Lenis, D. Petrellis, and P. A. Terziev, *Phys. Lett. B* **588**, 172 (2004).

- [6] R. F. Casten and N. V. Zamfir, *Phys. Rev. Lett.* **87**, 052503 (2001).
[7] R. Krücken *et al.*, *Phys. Rev. Lett.* **88**, 232501 (2002).
[8] D. Tonev, A. Dewald, T. Klug, P. Petkov, J. Jolie, A. Fitzler, O. Moller, S. Heinze, P. von Brentano, and R. F. Casten, *Phys. Rev. C* **69**, 034334 (2004).
[9] A. Dewald *et al.*, *J. Phys. G: Nucl. Part. Phys.* **31**, S1427 (2005).
[10] P. Petkov *et al.*, *J. Phys.: Conf. Ser.* **366**, 012036 (2012).

- [11] A. A. Raduta and P. Baganu, *J. Phys. G: Nucl. Part. Phys.* **40**, 025108 (2013).
- [12] A. A. Raduta, A. C. Gheorghe, P. Baganu, and A. Faessler, *Nucl. Phys. A* **819**, 46 (2009).
- [13] A. Gheorghe, A. A. Raduta, and A. Faessler, *Phys. Lett. B* **648**, 171 (2007).
- [14] A. A. Raduta, V. Ceausescu, A. Gheorghe, and R. M. Dreizler, *Nucl. Phys. A* **381**, 253 (1982).
- [15] A. A. Raduta and P. Baganu, *Phys. Rev. C* **83**, 034313 (2011).
- [16] F. Iachello and A. Arima, *The Interacting Boson Model* (Cambridge University Press, Cambridge, UK, 1987).
- [17] G. Gneuss and W. Greiner, *Nucl. Phys.* **171**, 449 (1971).
- [18] G. Dracoulis *et al.*, *J. Phys. G: Nucl. Phys.* **12**, L97 (1986).
- [19] G. D. Dracoulis, *Phys. Rev. C* **49**, 3324 (1994).
- [20] U. Garg *et al.*, *Phys. Lett. B* **180**, 319 (1986).
- [21] J. C. Walpe *et al.*, *Phys. Rev. C* **85**, 057302 (2012).
- [22] Liu Yuan *et al.*, *Chin. Phys. Lett.* **25**, 1633 (2008).
- [23] K. Nomura, T. Otsuka, R. Rodriguez-Guzman, L. M. Robledo, and P. Sarriguren, *Phys. Rev. C* **83**, 014309 (2011).
- [24] L. M. Robledo, R. Rodriguez-Guzman, and P. Sarriguren, *J. Phys. G: Nucl. Part. Phys.* **36**, 115104 (2009).
- [25] L. Wilets and M. Jean, *Phys. Rev.* **102**, 788 (1956).
- [26] L. Fortunato, *Eur. J. Phys. A* **26**, 1 (2005).
- [27] A. G. Ushveridze, *Quasi-exactly Solvable Models in Quantum Mechanics* (IOP, Bristol, 1994).
- [28] M. E. Rose, *Elementary Theory of Angular Momentum* (Wiley, New York, 1957).
- [29] A. A. Raduta, A. Gheorghe, and Amand Faessler, *J. Phys. G: Nucl. Part. Phys.* **31**, 337 (2005).
- [30] A. S. Davydov and G. F. Filippov, *Nucl. Phys.* **8**, 237 (1958).
- [31] J. Jolie and A. Linnemann, *Phys. Rev. C* **68**, 031301(R) (2003).
- [32] R. Fossion, D. Bonatsos, and G. A. Lalazissis, *Phys. Rev. C* **73**, 044310 (2006).
- [33] S.-C. Wu and H. Niu, *Nucl. Data Sheets* **100**, 483 (2003).
- [34] B. Singh and J. C. Roedinger, *Nucl. Data Sheets* **111**, 2081 (2010).
- [35] C. M. Baglin, *Nucl. Data Sheets* **111**, 275 (2010).
- [36] C. M. Baglin, *Nucl. Data Sheets* **99**, 1 (2003).
- [37] B. Singh, *Nucl. Data Sheets* **95**, 387 (2002).
- [38] B. Singh, *Nucl. Data Sheets* **99**, 275 (2003).
- [39] C. M. Baglin, *Nucl. Data Sheets* **113**, 1871 (2012).
- [40] B. Singh, *Nucl. Data Sheets* **107**, 1531 (2006).
- [41] H. Xiaolong, *Nucl. Data Sheets* **108**, 1093 (2007).
- [42] E. A. McCutchan, R. F. Casten, and N. V. Zamfir, *Phys. Rev. C* **71**, 061301(R) (2005).
- [43] E. A. McCutchan and N. V. Zamfir, *Phys. Rev. C* **71**, 054306 (2005).
- [44] M. Finger *et al.*, *Nucl. Phys. A* **188**, 369 (1972).
- [45] V. Ceausescu and A. A. Raduta, *Prog. Th. Phys.* **52**, 903 (1974).
- [46] A. A. Raduta *et al.*, *Phys. Rev.* **8**, 1525 (1973).
- [47] A. A. Raduta, C. Lima, and A. Faessler, *Phys. Lett.* **121B**, 1 (1983).
- [48] A. A. Raduta, C. Lima, and A. Faessler, *Z. Phys. A* **313**, 69 (1983).